ADVANCED MATERIALS
www.advmat.de

Photoswitchable Membranes Based on Peptide-Modified Nanoporous Anodic Alumina: Toward Smart Membranes for On-Demand Molecular Transport

Tushar Kumeria, Jingxian Yu, Mohammed Alsawat, Mahaveer D. Kurkuri, Abel Santos, Andrew D. Abell,* and Dusan Losic**

The controlled transport of molecules across membranes is central to nature (e.g., in protein channels and ion pumps) but also to many highly valuable applications such as desalination, on-demand drug delivery, chromatography, and others. Artificial nanoporous membranes provide an important tool for studying the mechanisms and dynamics associated with molecular transporting across a membrane. In particular, artificial membranes allow the study of membrane surface interactions, size-exclusion effects, and other key determinants of transmembrane molecular transport; while also providing an opportunity to control or regulate the molecular transport on demand.[1–3] A number of strategies have been developed to fabricate artificial membranes with tunable and controlled molecular transport properties.[1,4] The incorporation of responsive polymeric brushes or hydrogels onto porous membranes (i.e., nanoporous anodic alumina, porous polymers, porous silicon, and carbon nanotube membranes) is the most common one, which allows the preparation of smart membranes with stimuli responsive molecular transport properties.[4] It is noteworthy that polymer brushes respond to a broad range of possible external stimuli (i.e., thermal, electrical, light, ionic strength, and pH) with fast stimuli response and do not completely block the pores (i.e., under optimized grafting conditions).[5] Previous studies on photoresponsive membranes utilized photosensitive systems including azobenzene, triphenyl-methane and spiropyran based photochromes, photoresponsive liquid crystals, and photoresponsive polypeptides in combination with polymer or zeolite based membranes.[5b] These systems have been employed in gas and salt separation, pervaporation, reverse osmosis, photocontrolled viscosity modulation, colloidal stability, surface wettability, and solvent permeability.[5b] However, these examples did not give rise to a fully reversible transport performance and presented long response time, limiting their practical applicability.

Stimuli responsive polymers have been grafted on to nanoporous anodic alumina membranes (NAAMs) to allow controlled and responsive molecular and ionic transport with a focus on on-demand and actuated release of model drugs to target chronic diseases that require daily dosing (i.e., angina pectoris, migraine, or other hormone-related diseases).[5c,6] However, grafting of stimuli responsive polymer brushes generally involves modifying the top surface or the pore mouth of the NAAMs, resulting in minimal chemical interactions between transporting molecules and the grafted polymer (as the polymer brushes are not present throughout the nanochannels). Furthermore, the polymerization process used in their preparation often results in nonuniform polymer chains, leading to nonuniform distribution of pore diameter across the membrane and bulk material with inefficient swelling and de-swelling properties. Also, this leads to randomly organized functional groups, giving rise to poor immobilization efficiency for biosensing, filtration, and chromatography applications.[5b,7] NAAMs have been prepared by electrochemical anodization of aluminum and offer straight cylindrical nanopores with minimal tortuosity, controllable geometry and tunable surface chemistry.[8] An alternative approach to overcome the inherent limitations of polymer-based stimuli responsive membranes, while providing the practical and functional requirements for selective on-demand molecular transport applications, is to synthetically modify nanoporous membranes with optically switchable molecules. This study presents for the first time, a photo stimuli responsive membrane system based on NAAMs functionalized with an azobenzene-containing photoswitchable peptide (PSP). PSP molecules were selectively immobilized along the internal surface of the NAAM pores, in order to manipulate the effective pore diameter of the NAAMs, depending on their isomeric form. This pore diameter modulation then regulates the transport of model dye molecule (Rose Bengal (RosB)) across the PSP modified NAA membranes. Exposure to specific wavelengths of light (364 nm in this case) switches the azobenzene component of PSP from a *trans* to a *cis* isomer, such that the associated change in PSP geometry controls the pore diameter of NAAMs and hence the

T. Kumeria, M. Alsawat, Dr. M. D. Kurkuri, Dr. A. Santos, Prof. D. Losic
School of Chemical Engineering
The University of Adelaide
Adelaide SA-5005, Australia
E-mail: dusan.losic@adelaide.edu.au

Dr. J. Yu, Prof. A. D. Abell
ARC Centre of Excellence for Nanoscale BioPhotonics (CNBP)
School of Chemistry and Physics
The University of Adelaide
Adelaide SA-5005, Australia
E-mail: jingxian.yu@adelaide.edu.au; andrew.abell@adelaide.edu.au

Dr. M. D. Kurkuri
Centre for Nano and Material Sciences
Jain University
Jain Global Campus
Bangalore-562112, India

DOI: 10.1002/adma.201500473

ADVANCED MATERIALS
www.advmat.de

Materials Views
www.MaterialsViews.com

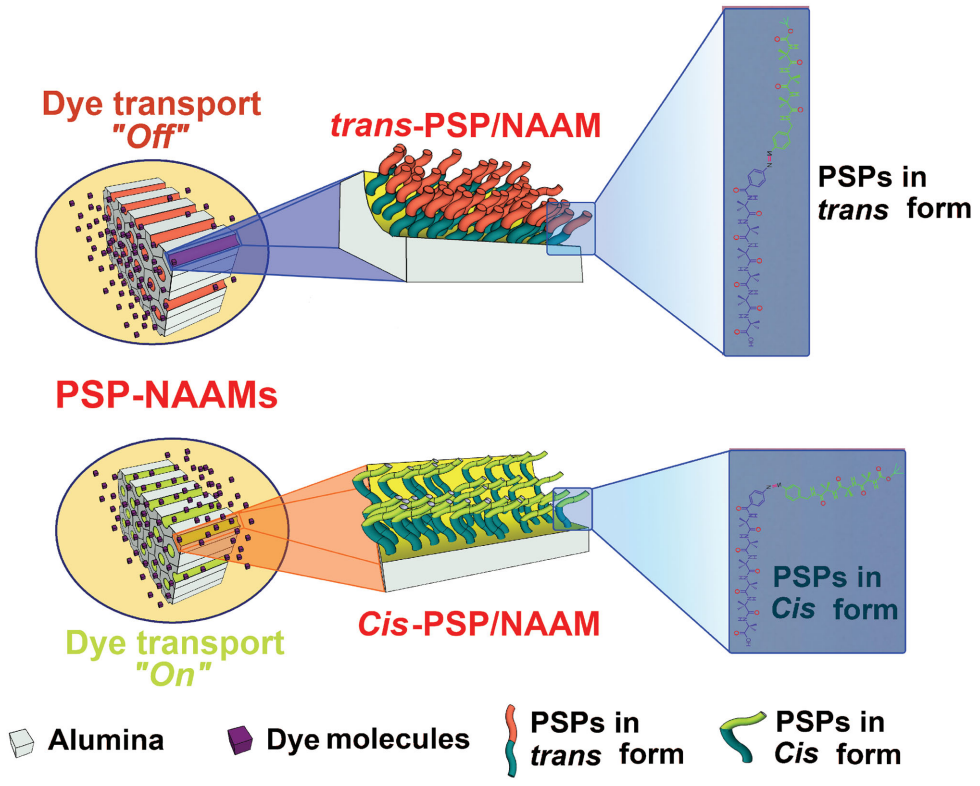

Figure 1. Schematic illustration of photoswitchable peptide-modified NAAMs (PSP-NAAMs), the transport properties of which were assessed by a U-tube permeation cell. PSP molecules in their *trans* or *cis* state effectively switch *Off* or *On*, respectively, which in turn regulates the molecular transport of a model dye molecule (RosB) through PSP-NAAMs.

selective transport of RosB, see **Figure 1**.[9,10] Photomediated switching of the PSP is experimentally confirmed by UV–Visible spectroscopy, contact angle measurements, atomic force microscopy (AFM), and molecular transport characterization including reversible *On*/*Off* switching of RosB transport across PSP/NAAMs as a function of PSP isomeric state (i.e., *cis* = *On* and *trans* = *Off*). A schematic illustration of the concept of photoregulated molecular transport through PSP-modified NAAMs is presented in Figure 1.

The photoswitchable peptide used in the study (**Figure 2**) consists of an azobenzene-derivative reversible light switch (4-aminomethyl phenylazobenzoic acid, Figure S1, Supporting Information), which is flanked by two Aib (α-aminoisobutyric acid) oligomers (Aib_3 and Aib_6) designed to help define the peptide geometry.[11] Aib oligomers were used specifically, since they are known to form predictable and stable helical structures, which are crucial for modulating the "effective pore diameter" in the NAAMs. The peptide was synthesized using the solid phase peptide synthesis (SPPS) procedure as detailed in the Supporting Information. This particular azobenzene derivative was chosen as the chromophore undergoes fast photocontrolled reversible isomerism, while remaining chemically stable.[10] An additional advantage of optically actuated switches is that they are nonresponsive to electromagnetic interference.[12] The resulting PSP compound was purified using reverse-phase high performance liquid chromatography (HPLC) and characterized using ^{1}H nuclear magnetic resonance spectroscopy (^{1}H NMR) (Figure S2, Supporting Information).

The photoisomerization of the PSP molecules was initially characterized by recording the UV–Vis spectrum after exposure to 440 and 364 nm wavelength lights. For this, first the PSP molecules were exposed to 440 nm wavelength of light for 10 min in order to give a photostationary state predominantly containing the *trans* PSP isomer. The absorption spectrum was then obtained which showed a strong band at 325 nm and a weak band at 430 nm (Figure 2a). The PSP solution was then illuminated at 364 nm to isomerize the *trans* isomer to the *cis*. A noticeable decrease in the peak at 325 nm was observed on exposing the PSP to 364 nm for 10 min (Figure 2a), which is consistent with formation of the *cis* isomer and the associated disappearance of the *trans* isomer. The switching between the isomers was found to be reversible, and it could be repeated for several cycles with complete recovery of the absorption signal. In order to define the backbone conformations of the peptide, the lowest energy conformers for both the *trans* and *cis* states of the photoswitchable compound **C1** were determined in Gaussian 09, with tight convergence criteria using a hybrid B3LYP method with 6–31G** basis set (Figure 2b,c). The molecular model predicts the length of the *trans* PSP structure to be ≈2.41 nm and 1.93 nm for the *cis* state.

Nanoporous anodic alumina membranes used in this work were fabricated through a two-step electrochemical anodization in 0.3 M sulfuric acid at 6 °C and 25 V, to obtain membranes with a nominal pore-channel diameter of 20 ± 3 nm (Supporting Information).[7] SEM images of NAAMs are depicted in **Figure 3**, where Figure 3a shows the top view of a

Adv. Mater. **2015**,
DOI: 10.1002/adma.201500473

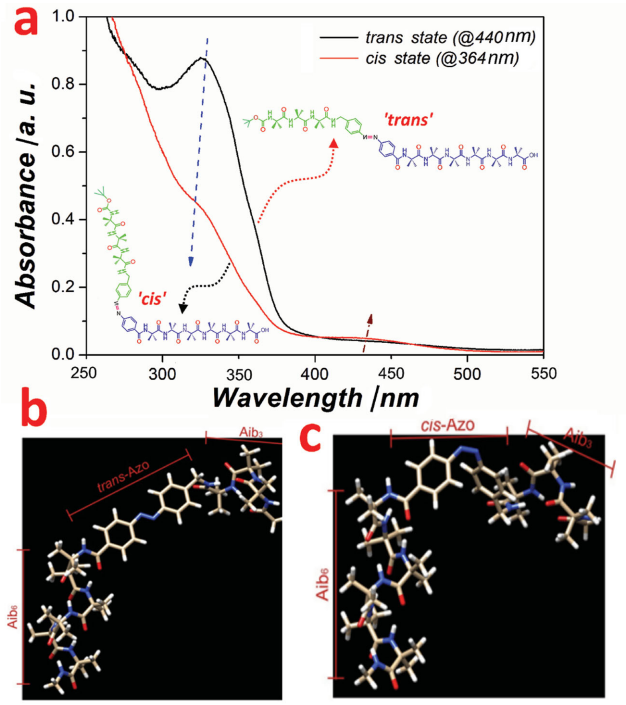

Figure 2. a) Absorbance spectrum of photoswitchable compound (i.e., PSP) under different isomeric states on exposure to specific wavelengths of light (with PSP isomeric structures inset). Computational models of photoswitchable peptide in its b) *trans* state and c) *cis* state.

NAAM and Figure 3b presents a cross-sectional view, with the inset showing perfectly straight and vertically aligned cylindrical nanopores. SEM images of the top and bottom surfaces of NAAMs, after pore opening using phosphoric acid (H_3PO_4 5 wt%) at 35 °C, are provided in Figure S3, Supporting Information, and show no damage to the top surface of NAAMs besides complete removal of barrier layer and in turn open pores at the bottom. Also, a digital photograph of the same NAAM sample (i.e., central transparent portion) is provided in Figure S3 inset, Supporting Information. Note that the thickness of NAAMs used for this study was fixed to 50 µm by adjusting the anodization time. Photoswitchable NAAMs were fabricated by covalent immobilization of PSP molecules onto 3-aminopropyl triethoxysilane (APTES) modified NAAMs.

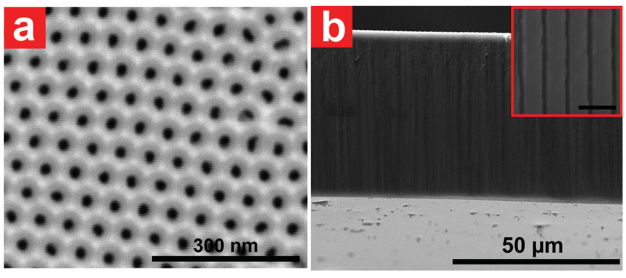

Figure 3. Typical SEM images of NAAM prepared in sulfuric acid electrolyte. a) Top view with self-organized pores. b) Cross-sectional view showing entire thickness of the NAAM with a magnified view inset (scale bar: 100 nm)

DIPEA/HATU (N,N-diisopropylethylamine/1-[bis(dimethylamino) methylene]-1H-1,2,3-triazolo[4,5-b]pyridinium3-oxid hexafluorophosphate) coupling reagents were used to form an amide linkage between carboxyl group on PSP molecules as well as acetic acid molecular spacer and amine group on APTES. This not only covalently couples PSP molecules to NAAMs inner surface, but also incorporates acetic acid spacers to ensure efficient and homogeneous switching PSP molecules between the two isomeric states (i.e., *trans* and *cis*) (Supporting Information).[13] Functionalization was confirmed by Fourier transform infrared (FTIR) and energy dispersive X-ray (EDX) spectroscopy as shown in Figure S4, Supporting Information. The FTIR spectrum for the APTES-NAAM and PSP/NAAM are shown in Figure S4a, Supporting Information, confirming successful functionalization of NAAMs with APTES and PSP molecules, respectively. The presence of a carbon peak for only the top surface of PSP/NAAMs in EDX spectra presented in Figure S4b, Supporting Information, confirms the selective attachment of PSP molecules on NAAMs.

Initially, the *cis*/*trans* switching capabilities of PSP molecules on a solid surface were examined by contact angle measurements after covalently attaching PSP molecules to silicon wafer surface using the aforementioned process. The PSP-modified Si wafers were first exposed to 364 nm light for 20 min to isomerize surface bound PSP to the *cis* isomer, and this was then subjected to water contact angle (WCA) measurements. Subsequent exposure to 440 nm light to enrich the *trans* PSP isomer on the Si surface was also followed by WCA measurements. The results shown in Figure S5a–c, Supporting Information, reveal an average WCA of 64° and 81° for PSP molecules in *trans* and *cis* states, respectively. The lower WCA for PSP molecules in the *trans* state is due to hydrophilic terminal group on the free end of PSP, whereas higher WCA for *cis* state is due to carbon backbone of the PSP molecules. This process was repeated three times to confirm the reversibility of the photoswitchable isomeric states of PSP molecules. The WCA measurements on NAAMs functionalized with PSP (Figure S5d, Supporting Information) displayed similar results to WCA measurements on Si wafer with an average WCA of 44° and 53° for *trans* and *cis* states of PSP molecules, respectively.

Next, we assessed the molecular transport performance of PSP modified NAAMs after exposure to 364 and 440 nm wavelength of light (i.e., PSP molecules under *cis* and *trans* isomeric states) using RosB as model molecule. This was examined by clamping PSP-modified membranes between two halves of a U-tube permeation unit composed of a feed and a permeate chamber (Figure S6, Supporting Information). The amount of RosB dye molecules transported was measured in real-time by following the changes in absorbance in the permeate chamber at 552 nm using a miniature fiber optical spectrometer (Supporting Information).[14] In this experiment, a PSP/NAAM was first exposed to 364 nm for 20 min in order to provide a photostationary state enriched in the *cis* azobenzene isomer (*cis*-PSP/NAAM). This *cis*-PSP/NAAM was then packed in the U-tube permeation cell and changes in absorbance of the RosB dye molecules in the permeate chamber were measured for 5 h. This was repeated with a PSP-modified NAAM, which had been exposed to 440 nm for 20 min in order to provide a photostationary state enriched in the *trans* azobenzene isomer

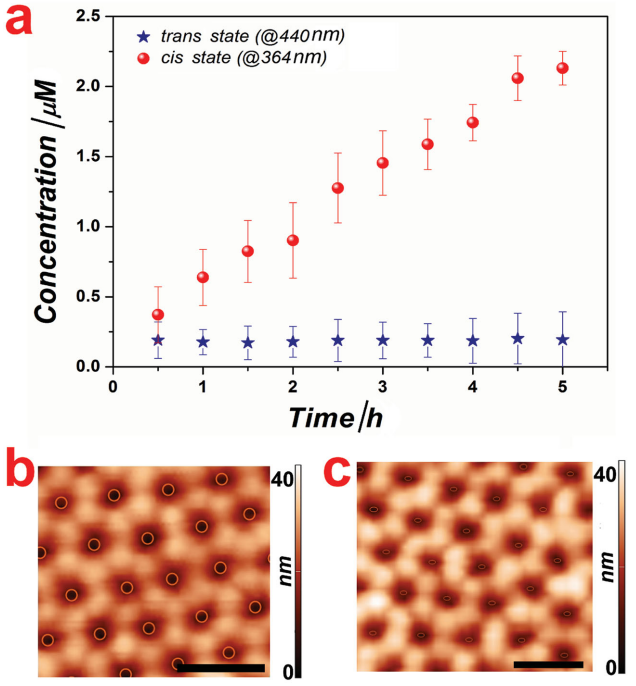

Figure 4. a) Molecular transport of dye (RosB) through PSP/NAAM under different isomeric states of PSP. AFM height images of PSP/NAAMs corresponding to its b) *cis* state and c) "*trans*" state of the PSP, respectively (scale bar: 100 nm).

(*trans*-PSP/NAAM) prior to transport analysis. **Figure 4**a shows changes in concentration of RosB in the permeate chamber for *cis*-PSP/NAAM and *trans*-PSP/NAAM systems. A linear increase in the concentration of RosB in the permeate chamber occurred for the *cis*-PSP/NAAM system. In contrast, the transport of RosB from the feed to the permeate chamber was greatly reduced for the *trans*-PSP/NAAM system. RosB concentrations of $0.194 \pm 0.0098 \times 10^{-6}$ M and $2.134 \pm 0.056 \times 10^{-6}$ M were obtained in the permeate chamber after 5 h, which corresponds to a permeation flux of 3.48×10^{-4} μmol h^{-1} cm^{-3} and 3.79×10^{-2} μmol h^{-1} cm^{-3} for *trans*-PSP/NAAM and *cis*-PSP/NAAM, respectively. Figure 4b,c shows AFM images of this system in the *cis*-PSP/NAAM and *trans*-PSP/NAAM configurations. The average pore diameter of *cis*-PSP/NAAM and *trans*-PSP/NAAM was 20 ± 3 nm and 13 ± 5 nm, respectively. These clearly show a significant change in the diameter of pores on exposure to 364 nm and 440 nm light, respectively, which are in good agreement with the obtained permeation flux data. Line section analysis of the AFM images is provided in Figure S7, Supporting Information, which shows that under *cis* photostationary state AFM can recognize the pore depth in more details as compared to the *trans* photostationary state of PSP/NAAM. The ability of this system to perform on-demand transport of dye molecules was then demonstrated by cyclic switching between the two photostationary states (i.e., *cis* and *trans*) of azobenzene group of PSP molecules grafted onto NAAMs surface. This was carried out by cyclic exposure of PSP/NAAM to 440 and 364 nm wavelengths of light and transport of RosB was monitored in real-time to measure the molecular transport rate. **Figure 5** shows transport of RosB across PSP/NAAM as

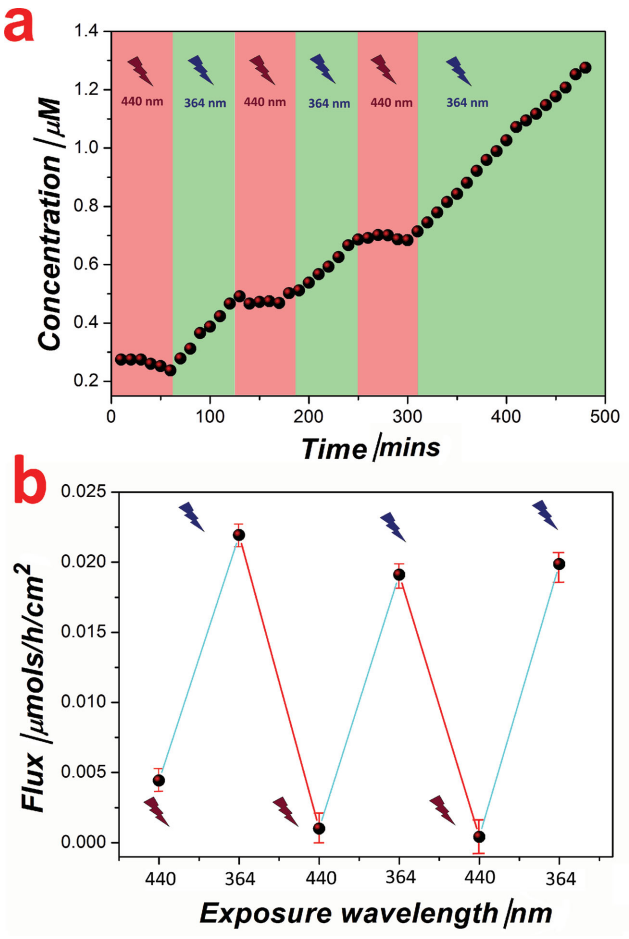

Figure 5. a) Molecular transport of dye (RosB) through PSP/NAAM after alternative exposure to 440 and 364 nm light. b) Flux of dye transport through PSP/NAAM as a function of different wavelengths of light.

a function of exposure to 364 and 440nm wavelength of light establishing the on-demand transport of dye molecules from the feed to the permeate chamber as a function of the exposure wavelength. The PSP/NAAM system was first exposed to 440 nm for 60 min, resulting in very low molecular transport. This was followed by exposure to 364 nm light, which resulted in a sharp increase in the concentration of dye in the permeate chamber (Figure 5a) presumably due to isomerism of *trans* to *cis* with an associated change in pore size. The RosB transport results (Figure 5) demonstrate that the proposed system is able to switch between *On* and *Off* states, thus allowing for on-demand transport of dye molecules. This system mimics a cell membrane's ability to control the transport the nutrients and molecules on demand. It clearly demonstrates its suitability for applications involving reversible transport. The trend for the flux data and is presented in Figure 5b showing the average flux for PSP/NAAM at 440 nm is 9.24×10^{-4} μmol h^{-1} cm^{-2} and 2.04×10^{-2} μmol h^{-1} cm^{-2} for 364 nm.

Note that, although the pores of PSP/NAAM were not completely closed on exposure to 440 nm, transport of dye molecules was effectively reduced, becoming almost negligible (Figure 4b). This suggests that the terminal groups (positively charged amine terminals) on PSP molecules immobilized onto

Adv. Mater. **2015**,
DOI: 10.1002/adma.201500473

the inner surface of NAAMs, also played a role in controlling the transport of dye molecules (negatively charged RosB). To confirm the role of electrostatic interaction on transport properties of RosB, the transport properties of a PSP/NAAMs with PSP molecules attached only on the pore mouths were analyzed (Supporting Information). To this end, a NAAM was selectively functionalized with an APTES layer on its top surface (5 μm; 10% of its total thickness – 50 μm). This membrane was prepared using a previously described process.[7c] The top 5 μm layer was then covalently modified with PSP molecules using the aforementioned functionalization procedure and subjected to RosB transport after exposure to 364 and 440 nm wavelength of light (i.e., at enriched *cis* and *trans* azobenzene photostationary states, respectively, (Figure S6b, Supporting Information)). The dye flux for NAAM having only top 5 μm PSP layer on exposure to 440 nm was measured at 3.0×10^{-3} μmol h^{-1} cm^{-2}, which is one order of magnitude faster than that obtained with *trans*-PSP/NAAM (i.e., on exposure to 440 nm wavelength of light) when the inner surface of the pores are entirely modified with PSP molecules. These results confirm that electrostatic interactions between the dye molecules and PSP molecules attached onto the inner surface of NAAM pores play a significant role in controlling the RosB transport. Therefore, the switchability of PSP/NAAMs is associated with a twofold effect; namely: (i) physical constriction of the nanopores and (ii) enhanced electrostatic interaction between positively charged PSP and negatively charged RosB molecules in synergy with pore diameter enlargement or constriction (i.e., molecular transport across PSP/NAAMs is governed by a combined effect of size exclusion and chemical interaction) (Figure S6b, Supporting Information). Furthermore, we assessed the effect of molecular spacers on efficiency of enrichment of a single photostationary state and hence, the transport properties of the proposed system. A schematic illustration of PSP immobilized inside NAAM with acetic acid spacers is provided in the Supporting Information along with the molecular size of acetic acid, RosB dye, APTES monolayer, and *cis* and *trans* photostationary states of PSP (Figure S8a, Supporting Information). To this end, another set of NAAMs were functionalized with PSP lacking the acetic acid spacer molecules and the transport of RosB dye molecules through these membranes was evaluated (Figure S8b, Supporting Information).[15] The average dye flux through these PSP/NAAMs was 2.58×10^{-2} μmol h^{-1} cm^{-2} at 440 nm exposure, which is about two orders of magnitude higher than that obtained when spacers are intercalated between PSP molecules. The transport of the same molecules through these PSP/NAAMs on exposure to 364 nm was determined to be 4.26×10^{-2} μmol h^{-1} cm^{-2}, which is almost two fold higher than that obtained when spacer molecules are intercalated between PSP molecules. The inferior RosB transport performance of the PSP/NAAMs, without spacers, could be due to the co-existence of both *cis* and *trans* photostationary states of azobenzene group on PSP, resulting in nonuniform interaction of dye molecules with the PSP and irregular diameter of the NAAMs pores. These results confirm that spacer molecules are essential to effectively enrich a single (i.e., *cis* or *trans*) photostationary state of azobenzene group on PSP molecules, which is in good agreement with previous studies.[14] Additionally, we studied the effect of the pore size of NAAMs. The transport of dye molecules through PSP-modified NAAMs featuring an average pore diameter of 35 nm, was found to be much slower than that of NAAMs with smaller pore diameters. Moreover, the control over switching of the transport of dye molecules was poor as it is dependent on the synergistic effect of pore size constriction and chemical interactions between dye and PSP molecules, which is in good agreement with the aforementioned results (Figure S8c, Supporting Information).

We also correlated the change in flux (J) and the pore diameter (d) according to a modified Hagen–Poiseuille equation defining the flux through a membrane with cylindrical straight pores as Equation (1) (Supporting Information)[6a]

$$\frac{J_2}{J_1} = \frac{d_2^4}{d_1^4} \tag{1}$$

where, the subscripts 1 and 2 represent the *trans* and *cis* states of photostationary state of azobenzene moiety on PSP, respectively. It is assumed that the change in thickness of PSP/NAAM is almost negligible in comparison to the change in pore diameter during switching between the two photostationary states (i.e., *cis* and *trans*) (Figure S9, Supporting Information). By substituting the values of the geometric features established from AFM and SEM analysis, $d_2 = 20$ nm (i.e., *cis* state) and $h_1 = h_2 =$ 50 000 nm, (Figures 3 and 4b,c) and $J_2/J_1 = 2.03 \times 10^{-2}/9.24 \times 10^{-4}$, d_1 (i.e., *trans* state) is calculated as 10 nm, which is close to the value measured by AFM (13 nm) (Figure 4c). This slight variation in the calculated (i.e., 10 nm) and experimentally determined pore diameter (i.e., 13 nm) is likely due to the Hagen–Poiseuille equation used to calculate the pore diameter, which does not account for the electrostatic interactions between the dye molecules and PSP groups inside NAAM pores.

Kinoshita and co-workers developed a range of photoswitchable polypeptide based stimuli responsive membranes systems using polymer membranes (mostly poly(L-glutamic acid) membrane). These photoresponsive membranes were employed for controlled ionic transport targeting desalination and reverse osmosis application. However, the transport properties of these membranes were irreversible and dependent on external factors (i.e., pH, temperature and others).[5b-f] Notice that, the use of PSP, a photoswitchable peptide composed of 4-aminomethyl phenylazobenzoic acid molecules sandwiched between two Aib (α-aminoisobutyric acid) oligomers (Aib3 and Aib6), into a membrane system with fully controllable and reversible molecular transport properties is a unique and exclusive characteristic of the presented study. In this regard, Table S1, Supporting Information, summarizes and compares the performance of previously reported photoswitchable membranes to the PSP/NAAMs presented in this study.

In conclusion, novel functional membranes with capabilities of controlled and on-demand molecular transport were developed using photoswitchable peptides and nanoporous anodic alumina membranes. The photoregulated molecular transport properties of these structures were assessed using model molecule (Rose Bengal dye). The molecular transport across photoswitchable peptide-modified nanoporous anodic alumina membranes (PSP-NAAMs) system can be reversibly and cyclically actuated by switching the photostationary state of the azobenzene unit on PSP molecules. The controlled transport of

RosB molecules is based on synergy between the size-exclusion effects and affinity between dye molecules and surface chemistry on PSP/NAAMs. The on-demand photostationary state switching response time of PSP molecules was found to be less than 10 min, and thus on-demand regulation in this system is possible by optical stimulation. Given these promising results, we suggest that this system could be applied for water purification and various biotechnological applications.

Supporting Information

Supporting Information is available from the Wiley Online Library or from the author.

Acknowledgements

M.D.K. and A.S. contributed equally to this work. Authors acknowledge the financial support provided by the Australian Research Council (ARC) Centre of Excellence for Nanoscale BioPhotonics (CNBP), the Australian Research Council (DP 120101680, FT 110100711, and DE14010054), Centre for Advanced Nanomaterials (CAN) at The University of Adelaide, School of Chemical Engineering and Department of Chemistry at The University of Adelaide. The computational aspects of this work were supported by an award under the National Computational Merit Allocation Scheme for J.Y. on the National Computing Infrastructure (NCI) National Facility at the Australian National University and M.D.K. also acknowledge Department of Science and Technology (DST/TM/WTI/2K14/213), India for financial support.

Received: January 29, 2015
Revised: March 17, 2015
Published online:

[1] a) K. B. Jirage, J. C. Hulteen, C. R. Martin, *Science* **1997**, *278*, 655; b) B. B. Lakshmi, C. R. Martin, *Nature* **1997**, *388*, 758; c) J. Wu, K. Gerstandt, H. Zhang, J. Liu, B. J. Hinds, *Nat. Nanotechnol* **2012**, *7*, 133; d) M. Majumder, N. Chopra, B. J. Hinds, *J. Am. Chem. Soc.* **2005**, *127*, 9062; e) M. Majumder, N. Chopra, B. J. Hinds, *ACS Nano* **2011**, *5*, 3867; f) S. Szobota, E. Y. Isacoff, *Annual Rev. Biophys.* **2010**, *39*, 329; g) C. R. Martin, M. Nishizawa, K. Jirage, M. Kang, S. B. Lee, *Adv. Mater.* **2001**, *13*, 1351.

[2] a) K. H. Wee, R. Bai, E. M. V. Hoek, V. V. Tarabara, *Encyclopedia of Membrane Science and Technology*, John Wiley & Sons, Inc., Hoboken, NJ **2013**; b) D. Wandera, S. R. Wickramasinghe, S. M. Husson, *J. Membrane Sci.* **2010**, *357*, 6; c) S. M. Webster, D. del Camino, J. P. Dekker, G. Yellen, *Nature* **2004**, *428*, 864.

[3] a) S. B. Lee, C. R. Martin, *J. Am. Chem. Soc.* **2002**, *124*, 11850; b) R. Karnik, R. Fan, M. Yue, D. Li, P. Yang, A. Majumdar, *Nano Lett.* **2005**, *5*, 943.

[4] a) H. Alem, A. S. Duwez, P. Lussis, P. Lipnik, A. M. Jonas, S. Demoustier-Champagne, *J. Membrane Sci.* **2008**, *308*, 75; b) F. Liu, C. H. Du, B. K. Zhu, Y. Y. Xu, *Polymer* **2007**, *48*, 2910; c) S. J. Lue, J. J. Hsu, T. C. Wei, *J. Membrane Sci.* **2008**, *321*, 146.

[5] a) R. B. Vasani, S. J. McInnes, M. A. Cole, A. M. M. Jani, A. V. Ellis, N. H. Voelcker, *Langmuir* **2011**, *27*, 7843; b) F. P. Nicoletta, D. Cupelli, P. Formoso, G. De Filpo, V. Colella, A. Gugliuzza, *Membranes* **2012**, *2*, 134; c) T. Kinoshita, M. Sato, A. Takizawa, Y. Tsujita, *J. Chem. Soc. Chem. Commun.* **1984**, *14*, 929; d) T. Kinoshita, M. Sato, A. Takizawa, Y. Tsujita, *Macromolecules* **1986**, *19*, 51; e) T. Kinoshita, M. Sato, A. Takizawa, Y. Tsujita, *J. Chem. Soc. Chem. Comm.* **1986**, *108*, 6399; f) M. Sato, T. Kinoshita, A. Takizawa, Y. Tsujita, *Macromolecules* **1988**, *21*, 3419; g) S. K. Kumar, J. D. Hong, *Langmuir* **2008**, *24*, 4190.

[6] a) G. Jeon, S. Y. Yang, J. Byun, J. K. Kim, *Nano Lett.* **2011**, *11*, 1284; b) C. Song, W. Shi, H. Jiang, J. Tu, D. Ge, *J. Membrane Sci.* **2011**, *372*, 340; c) P. F. Li, R. Xie, J. C. Jiang, T. Meng, M. Yang, X. J. Ju, L. Yang, L. Y. Chu, *J. Membrane Sci.* **2009**, *337*, 310.

[7] a) T. Kumeria, M. Bariana, T. Altalhi, M. Kurkuri, C. T. Gibson, W. Yang, D. Losic, *J. Mater. Chem. B* **2013**, *1*, 6302; b) C. Tao, J. Wang, S. Qin, Y. Lv, Y. Long, H. Zhu, Z. Jiang, *J. Mater. Chem.* **2012**, *22*, 24856; c) T. R. Hoare, D. S. Kohane, *Polymer* **2008**, *49*, 1993.

[8] a) O. Jessensky, F. Müller, U. Gösele, *Appl. Phys. Lett.* **1998**, *72*, 1173; b) H. Masuda, K. Fukuda, *Science* **1995**, *268*, 1466; c) A. M. M. Jani, I. M. Kempson, D. Losic, N. H. Voelcker, *Angew. Chemie* **2010**, *122*, 8105.

[9] O. Babii, S. Afonin, M. Berditsch, S. Reiβer, P. K. Mykhailiuk, V. S. Kubyshkin, T. Steinbrecher, A. S. Ulrich, I. V. Komarov, *Angew. Chemie Int. Ed.* **2014**, *53*, 3392.

[10] a) M. M. Russew, S. Hecht, *Adv. Mater.* **2010**, *22*, 3348; b) Y. J. Liu, G. Y. Si, E. S. Leong, N. Xiang, A. J. Danner, J. H. Teng, *Adv. Mater.* **2012**, *24*, 131; c) Y. B. Zheng, B. K. Pathem, J. N. Hohman, J. C. Thomas, M. Kim, P. S. Weiss, *Adv. Mater.* **2013**, *25*, 302; d) S. L. Chen, C. C. Chu, V. K. S. Hsiao, *J. Mater. Chem. C* **2013**, *1*, 3529.

[11] a) S. Zhu, M. Riou, C. A. Yao, S. Carvalho, P. C. Rodriguez, O. Bensaude, P. Paoletti, S. Ye, *Proc. Natl. Acad. Sci. USA* **2014**, *111*, 6081; b) A. A. Beharry, O. Sadovski, G. A. Woolley, *J. Am. Chem. Soc.* **2011**, *133*, 19684.

[12] A. L. Ricchiuti, D. Barrera, K. Nonaka, S. Sales, *Opt. Lett.* **2014**, *39*, 5729.

[13] a) A. Adochitei, G. Drochioiu, *Rev. Roum. Chim.* **2011**, *56*, 783; b) T. Kumeria, A. Santos, D. Losic, *ACS Appl. Mater. Interfaces* **2013**, *5*, 11783.

[14] a) T. Altalhi, M. Ginic-Markovic, N. Han, S. Clarke, D. Losic, *Membranes* **2010**, *1*, 37; b) T. Altalhi, T. Kumeria, A. Santos, D. Losic, *Carbon* **2013**, *63*, 423.

[15] D. T. Valley, M. Onstott, S. Malyk, A. V. Benderskii, *Langmuir* **2013**, *29*, 11623.